Journal Pre-proof

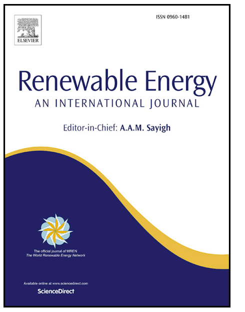

Modeling of solar-assisted ground-coupled heat pumps with or without batteries in remote high north communities

Florian Maranghi, Louis Gosselin, Jasmin Raymond, Martin Bourbonnais

PII: S0960-1481(23)00326-9

DOI: https://doi.org/10.1016/j.renene.2023.03.040

Reference: RENE 18495

To appear in: *Renewable Energy*

Received Date: 7 June 2022

Revised Date: 29 December 2022

Accepted Date: 8 March 2023

Please cite this article as: Maranghi F, Gosselin L, Raymond J, Bourbonnais M, Modeling of solar-assisted ground-coupled heat pumps with or without batteries in remote high north communities, *Renewable Energy* (2023), doi: https://doi.org/10.1016/j.renene.2023.03.040.

Florian Maranghi : Conceptualization; Methodology; Software; Validation; Writing - Original Draft;

Louis Gosselin : Conceptualization; Methodology; Validation; Resources; Writing - Review & Editing; Supervision

Jasmin Raymond : Conceptualization; Writing - Review & Editing; Funding acquisition; Supervision

Martin Bourbonnais : Writing - Review & Editing

MODELING OF SOLAR-ASSISTED GROUND-COUPLED HEAT PUMPS WITH OR WITHOUT BATTERIES IN REMOTE HIGH NORTH COMMUNITIES

Florian Maranghi[1], Louis Gosselin[1,*], Jasmin Raymond[2], Martin Bourbonnais[3]

[1]Department of Mechanical Engineering, Université Laval, Quebec City, Quebec, G1V 0A6, Canada

[2]Institut national de la recherche scientifique (INRS), Centre Eau Terre Environnement, Quebec City, Quebec G1K 9A9, Canada

[3]Cégep de Jonquière, Centre des technologies des énergies renouvelables et du rendement énergétique, Saguenay, G7X 7W2, Canada

Abstract

Many subarctic communities rely entirely on fossil fuels for their energy needs. Solar-assisted ground-coupled heat pumps (SAGCHP) can be a solution to integrate renewable energy sources into their energy portfolios. However, it is currently unknown how such systems could operate in the context of the high North (cold ground, extreme mismatch between insolation and heating need, electricity from diesel). The objective of the paper is to develop a detailed model of a SAGCHP heating a house in Nunavik (Quebec, Canada) in order to gain a better understanding of its potential and limitations. The solar assistance is provided by PVs. Simulations with and without electric storage (batteries) were run. A complex tradeoff between four different modes of operation was obtained depending on the conditions of the system at each time step. For the test case, results show that the ground experiences a weak long-term thermal depletion partly compensated solar energy, but that a significant portion of the PV power production is preferably used by the compressor or stored in batteries rather than stored in the ground as heat. Over ten years, the SAGCHP system reduced fuel consumption respectively by 38.2% (without a battery) and 59.1% (with a battery).

* Corresponding Author: Louis.Gosselin@gmc.ulaval.ca

Keywords: geothermal; ground heat exchanger; subarctic building; photovoltaic; renewable energy; energy storage.

Nomenclature

COP	Heat pump coefficient of performance [-]
$C_{p,f}$	Specific heat capacity of heat transfer fluid [J/(kg.K)]
$E_{change,battery}$	Battery energy change at the end of a ten-year operation [MJ]
$E_{change,borefield}$	Borefield energy change at the end of a ten-year operation [MJ]
$E_{change,tank}$	Storage tank energy change at the end of a ten-year operation [MJ]
$E_{elec,HP}$	Electrical energy consumed by the heat pump during a ten-year operation [MJ]
$E_{elec,pump}$	Electrical energy required for the circulation pump to move the fluid in the GHE during a ten-year operation [MJ]
$E_{loss,borefield}$	Heat transferred from the borefield to the environment through its top, lateral and bottom sides during a ten-year operation [MJ]
$E_{loss,tank}$	Heat transferred from the storage tank to the environment during a ten-year operation [MJ]
$E_{x\rightarrow y}$	Energy (heat or electrical) transferred from component *x* to component *y* (or group of components *y*) during a ten-year operation [MJ]
FS	Total diesel savings performed with the use of a SAGCHP [-]
H_{header}	Ground heat exchanger header depth [m]
k_g	Ground thermal conductivity [W/(m.K)]
LHV	Diesel lower heating value [MJ/L]
$\dot{m}_f$	Mass flow rate of heat transfer fluid [kg/s]
$P_{battery\rightarrow HP}$	Electrical power supplied to the heat pump by the battery [W]
$P_{elec,HP}$	Electrical power consumed by the heat pump [W]
$P_{elec,pump}$	Electrical power consumed by the pump [W]
$P_{fluid\rightarrow HP}$	Heat transfer rate from the fluid to the heat pump [W]
P_{GHE}	Potential heat transfer rate from the storage tank to the ground during operation mode 2 [W]
$P_{ground\rightarrow fluid}$	Heat transfer rate from the ground to the fluid [W]
P_{PV}	Electrical power produced by the PV [W]
$P_{PV\rightarrow battery}$	Electrical power supplied to the battery [W]
$P_{PV\rightarrow HP}$	Electrical power supplied to the heat pump by the PV [W]
$P_{PV\rightarrow pump}$	Electrical power supplied to the circulation pump by the PV [W]

$P_{PV \rightarrow tank}$	Electrical power supplied to the storage tank by the PV [W]
$P_{tank \rightarrow GHE+HP}$	Heat transfer rate from the storage tank to the ground or the heat pump [W]
SOC	Battery fractional state of charge [-]
t	Current simulation time step [h]
T_a	Atmospheric temperature [°C]
$T_{borefield}$	Average temperature of the ground volume around the boreholes [°C]
T_g	Undisturbed ground temperature [°C]
$T_{in,GHE}$	Fluid temperature entering the GHE [°C]
$T_{in,HP}$	Fluid temperature entering the HP [°C]
$T_{out,GHE}$	Fluid temperature exiting the GHE [°C]
$T_{out,HP}$	Fluid temperature exiting the HP [°C]
$T_{out,tank}$	Fluid temperature exiting the storage tank [°C]
T_{tank}	Average fluid temperature in the storage tank [°C]
T_{s1}	Temperature of the surface of the ground in the borefield [°C]
T_{s2}	Temperature of the surface of the ground around the borefield [°C]
U	Global heat transfer coefficient between the ground surface and the atmosphere [W/(m².K)]

Greek Symbols

$\eta_{furnace}$	Oil-furnace global efficiency [-]
$\eta_{power\ plant}$	Diesel power plant global efficiency [-]

Acronyms

ASHRAE	American Society of Heating, Refrigerating and Air-Conditioning Engineers
COP	Coefficient of performance
DHW	Domestic hot water
GCHP	Ground-coupled heat pump
GHE	Ground heat exchanger
HDPE	High-density polyethylene
HP	Heat pump
MPP	Maximum power point
MPPT	Maximum power point tracker
n/B	Scenario without battery

PV	Photovoltaic (photovoltaic panels)
SAGCHP	Solar-assisted ground-coupled heat pump
TMY	Typical meteorological year
TRNSYS	TRaNsient SYstems Simulation Program
w/B	Scenario with battery

1. Introduction

There are many isolated and remote communities all over the world. For example, there are 292 such communities in Canada, many of which are located in the Northern part of the country [1]. Due to their remoteness, most villages are not connected to the main power grid and rely on local diesel power plants for electricity. Furthermore, fuel oil is used for space heating. The complete dependency on fossil fuels can be seen as problematic due to the high and volatile cost of energy, the greenhouse gas emissions of fuels, the noise, and the risks of spills. In Nunavik, the northern portion of the province of Quebec (Canada), the cost of electricity generation lied between 0.65 CAD/kWh and 1.324 CAD/kWh (before subsidy) in 2013 [2], and the price of fuel oil reached 2.03 CAD/L in 2018 (before subsidy) [3], [4]. Communities and governments are now looking for options to integrate renewable energy sources into the local energy mix of northern off-grid villages, taking into account their climatic, social and environmental specificities [1], [2]. Solar energy can be a promising option. However, the mismatch between the energy demand and the production is a major issue and calls for the use of energy storage. At such latitudes, days are extremely short in the winter and long in the summer. One of the options currently under investigation in Nunavik is the integration of photovoltaic panels with ground heat exchangers and heat pumps, relying on the ground for short and long-term heat storage.

Recent studies have investigated the ability of ground-coupled heat pump systems (GCHP) to provide space heating in Nunavik. Among the main challenges encountered are the low temperature of the ground, the absence of cooling load in the summer (i.e., there is no thermal recharge of the ground), and the cost and environmental footprint of the electricity required to operate the compressor since it comes from diesel generators. Evaluations of the geothermal potential of Nunavik (Quebec, Canada) were carried out: Comeau et al. extrapolated the ground temperature profile and mapped the distribution of the ground thermal conductivity in the province of Québec. Their work was based on the ground thermal properties of 28 geothermal sites and on the geological data of the province [5]. Giordano et al. conducted surveys in the community of Kuujjuaq (Nunavik). Their study provides thermal conductivities and capacities of the ground subsurface [6]. Belzile et al. simulated a GCHP with horizontal exchangers in Kangiqsualujjuaq and demonstrated that it was possible to reduce fuel oil consumption by 40% with a ground-coupled absorption heat pump [7]. However, their study also concluded that ground-coupled heat pumps consume more energy and fuel to heat the building than a furnace when the heat pump is supplied with electricity produced from diesel or directly driven by a diesel engine. It should be noted that their study considers the use of customized heat pumps able to handle fluid temperatures as low as -14 °C. Giordano and Raymond simulated a five-year operation of a borehole storage system for a drinking water facility in Kuujjuaq [8]. Giordano et al. simulated vertical ground heat exchangers (GHE) for ten years. They showed that it was possible to extract 35 W/m from the ground for nine months of each year with 30 m-deep boreholes, when considering a minimum ground heat exchanger temperature of -10 °C [9]. Gunawan et al. assessed the geothermal potential in the community of Kuujjuaq and performed an economic analysis of several energy scenarios [3]. Despite the unfavorable Nunavik's conditions described earlier, their study reveals that all GCHP options can be economically attractive compared to fuel oil furnaces over a 50-year horizon. It also highlighted the economic benefits of consuming electricity from solar photovoltaic panels to run the system, rather than electricity from the community grid.

A few examples of successful GCHP projects in cold climates can be found in the literature. The report from Meyer et al. provides a literature review of systems operating in Alaska (USA) that meet the heating demand and allow to save costs over other heating systems [10]. Cost analyses proved that GCHP could be economically viable in Alaska, and that this viability depends on the price of the electricity consumed to run the GCHP and the price of fuel that is being replaced. Garber-Slaght et al. noted that GCHP are cost effective when cheap electricity meets expensive fuel oil, for the case studied in Fairbanks [11]. However, Meyer et al. point out that GCHP could be inadequate in some areas of Alaska because of their high operational and installation costs [10].

One of the major issues with GCHP in heating dominated areas is the unbalanced load imposed to the ground. This could result in excessive ground thermal depletion and the degradation of the heat pump performance over the years [11], [12]. For this reason, Garber-Slaght et al. pointed out the lack of long-term studies of GCHP in heating dominated climates, and the need to study the evolution of their performance over their entire lifetime. Studies investigated several ways to deal with this long-term thermal depletion. It appears that improving the borefield layout, increasing the spacing between the boreholes and increasing the exchanger length (greater number of boreholes and deeper boreholes) can help the ground to recover faster and could be sufficient to handle slight thermal imbalances [12], [13]. High ground thermal properties (thermal conductivity, thermal diffusivity), high moisture content and the possibility of freezing the ground water content are also favorable [14], [15]. In other cases, thermal depletion is not expected when significant groundwater flow is present as it contributes to the thermal recharge of the borefield. However, when the thermal imbalance is severe, the use of a secondary source of heat and the use of seasonal thermal storage become appropriate solutions, according to You et al. [16].

Several studies investigated the integration of auxiliary sources of energy to reduce the ground thermal imbalance [12]. Among solutions, the technology known as solar-assisted ground-coupled heat pump (SAGCHP) integrates solar energy by using solar thermal collectors or photovoltaic panels with the geothermal system. Solar energy can serve different purposes. For instance, it can reduce ground heat extraction when serving as a source of heat for direct production of domestic hot water (DHW) or for direct space heating [12]. When connected with the GHE and the heat pump, the solar assistance can serve as a heat source to raise the temperature of the fluid entering the heat pump and then increase its coefficient of performance (COP). When connected with the GHE, the solar assistance can recharge the ground through heat storage [17]. This last purpose can be declined in several applications. Seasonal heat storage can occur at relatively low temperatures with the aim to compensate for the yearly thermal imbalance and eventually slightly increase the temperature of the fluid entering the heat pump and, thus, its COP. Heat storage can also be done at high temperatures, but this requires an underground storage volume with insulated boundaries [18].

The studies from Kjellsson et al. question the benefits of underground seasonal storage [19], [20]. They performed TRNSYS simulations of a SAGCHP located in Stockholm, Sweden, using solar collectors and a short-term storage tank. The configuration of the system allowed three main operation scenarios. The collectors can provide only DHW, or they can provide heat to the boreholes and then, recharge the ground and increase the fluid temperature in the evaporator, or they can perform both functions. In this last scenario, DHW production with solar heat and injection of solar heat in the borefield occur respectively during summer and winter. The authors compared these three scenarios, considering the electricity consumption (consumed to run the circulating pumps, heat pump and auxiliary heating unit) and the space heating provided. According to their study, the recharge of the borefield must coincide with or be as close as possible from the ground heat extraction periods. Ground recharging is the most efficient in winter, when the weather conditions require most of the heat pump heating capacity and when its electricity consumption is likely to increase, because of the low borehole temperatures. During summer, if the system is sufficiently large, the solar heat must be used for DHW rather than for the recharge of the borefield, due to the heat losses that would occur in the ground over time. The recharge of the borefield in summer allows limited annual electricity savings through the improvement of the heat pump COP, unlike the production of solar DHW. On the contrary, the study from Zhu et al. reveals that solar energy can help prevent the long-term degradation of the heat pump COP while reducing the system operation cost and allowing a sustainable payback period, despite the additional cost of solar assistance [21]. In addition, Nordgård-Hansen et al. studied the optimization of systems including PVs, batteries and GCHPs. The energy needs of the GCHPs and dwellings did not always match the PV production. Thus, a part of it was used to perform ground heat injection, enabling the ground to reach near long-term thermal balance [22]. Such studies provide interesting insights but may not strictly apply to the subarctic climate where the undisturbed ground temperature is near the freezing point.

As can been seen from the literature review, there is evidence suggesting that GCHP could offer an opportunity to address some of the energy issues of communities such as those from the Canadian north and that solar assistance could alleviate problems such as the long-term thermal depletion due to the absence of a cooling load, the low ground temperature, and the environmental footprint of the electricity. However, at this point, it is unclear how such a system could actually work, and in particular, the performance that it could reach, as no assessment is available. A knowledge gap on the best technologies to be adopted for the Nunavik and other off-grid communities must be addressed. The objective of the present work is thus to develop a better understanding of how a SAGCHP system would work in the subarctic context. In order to do so, we developed a model of the SAGCHP system and a real house that it could service (Section 2) with TRNSYS. The house is located in the community of Whapmagoostui (Quebec, Canada) and energy bills were available to calibrate the building model. Only PV was considered for solar assistance due to local constraints preventing the use of thermal solar technologies. The model was then used to study the evolution of the fluid and ground temperatures, the energy flows in the system and the control of the system. Different scenarios were investigated, including the use of batteries for storing electricity and the way in which the electricity produced by the PV arrays is used.

2. Methodology

2.1 Space-heating load profile

In order to simulate the operation of a SAGCHP system, a heating demand profile is needed at a high temporal resolution. We generated this load profile from an energy model of a house located in the village of Whapmagoostui (Quebec, Canada) at a latitude of 55° 16’ North and a longitude of 77° 44’ West. This house is part of a research station of the Centre d’études nordiques (CEN). The roof of the building is composed of two sides oriented toward North and South with a tilt angle of 18°. The one-story building has a floor surface area of 94 m² with a crawl space. Overall, the window-to-floor ratio is 10%. The heating need of the building is currently satisfied by a forced-air fuel oil furnace, with an estimated efficiency of 80%. Typically, one person occupies this dwelling.

An energy model of the building was developed in TRNSYS. *Type 56*, *type 121a* and *type 75b* were used to respectively model the building, fuel oil furnace, and infiltrations. The required meteorological information was assembled from different sources: atmospheric pressure, wind speed, dry bulb temperature, relative humidity from [23], solar radiation from [24] and ground temperature at 2 cm from the surface [25].

Fig. 1. House of the CEN research station in Whapmagoostui (Quebec, Canada) serving as a test case for this project.

The model was calibrated with the fuel oil and electricity bills of 2017 and 2018. The fuel oil bills were used to calibrate the model parameters and generate a heating demand that matched the house consumption. First, the monthly electricity bills were used to adjust the heat gains associated with electrical devices in the model. Then, several model parameters were adjusted to match the average simulated fuel oil consumption with the bills, including the thermal resistance of the walls, doors, floor and roof, the equivalent air leakage area, the fraction of the consumed electricity transferred into internal gains, and the indoor setpoint temperature. It should be noted though that the fuel oil invoices were not issued every month, but rather every time the tank was refueled (periods ranging from 12 days to 153 days). Furthermore, according to the managing team of the station, the actual occupancy of the house over the two-year period varied, but no data was available on whether the house was occupied or not during specific days and if so, by how many people. Therefore, it was not possible to calibrate the model by following the requirements from ASHRAE Guideline 14-2002 [26]. However, it should be reminded that the objective of the present work is not to obtain an exact energy consumption profile of a given building, but rather to generate a realistic heating load profile for the purpose of analyzing the SAGCHP.

The calibrated model was then used to generate a typical yearly heating load profile (which will be used below to simulate the SAGCHP). Due to the absence of a Typical Meteorological Year (TMY) weather data file for Whapmagoostui, we analyzed weather data from different years to select a typical year for the purpose of the present work. As a first approximation, it is assumed that colder or cloudier years would balance out warmer or sunnier years which would not impact significantly the long-term ground thermal imbalance and SAGCHP performance. Therefore, we used a single typical year to model the conditions under which the system operates in the long-term (ten years). The yearly average solar irradiance and outdoor temperature were calculated from 2006 to 2019. The weather conditions of 2012 were found to be the closest to these averages and were thus retained for this paper. The space heating load profile was thus generated with the model described above for that specific year, as shown in Fig. 2. Even though only the daily average is reported in that figure for the sake of clarity, the heating need is available every ten-minute period from the simulation. Shorter time steps were tested and did not significantly change the results. In the rest of the present work, that load is used to represent the heating demand profile. The overall energy consumption for space heating is around 107 GJ/y, which corresponds to an annual heating intensity of 316 kWh/m^{2}y. Such an intensity is typical in Nunavik.

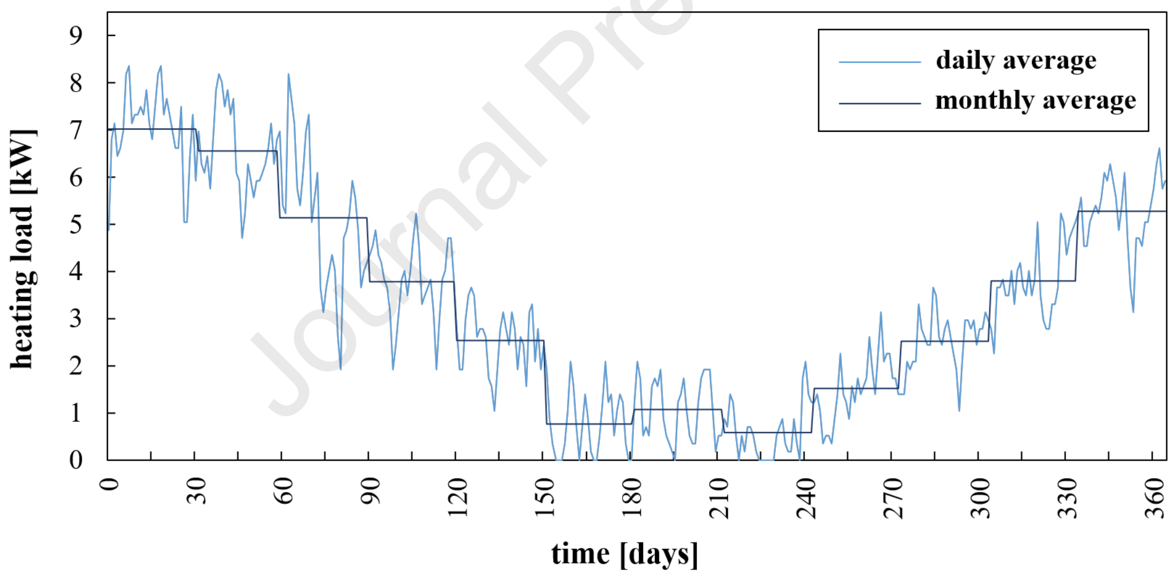

Fig. 2. Evolution of the daily and monthly average heating load of the residential building under study.

2.2 Description of the SAGCHP configuration

Fig. 3 shows the proposed SAGCHP configuration. It includes a water source heat pump operating parallel with the building fuel oil furnace. The borefield contains vertical ground heat exchangers (GHE) with U-pipes. Solar assistance is provided by photovoltaic panels (PV) which can feed the compressor of the heat pump (HP) or an electric resistance to warm up the fluid in a short-term storage tank. We assumed that the photovoltaic panels operated with a maximum power point tracking (MPPT) system. Four valves control the circulation of the fluid in the components. It is important to explain that solar thermal collectors are typically considered as an unsuitable solution to the Nunavik context due to costs (transportation, installation, maintenance), absence of qualified local personnel to maintain and repair them, harsh climatic conditions and low social acceptance. That is why it was decided to orient the present study on the use of photovoltaic panels.

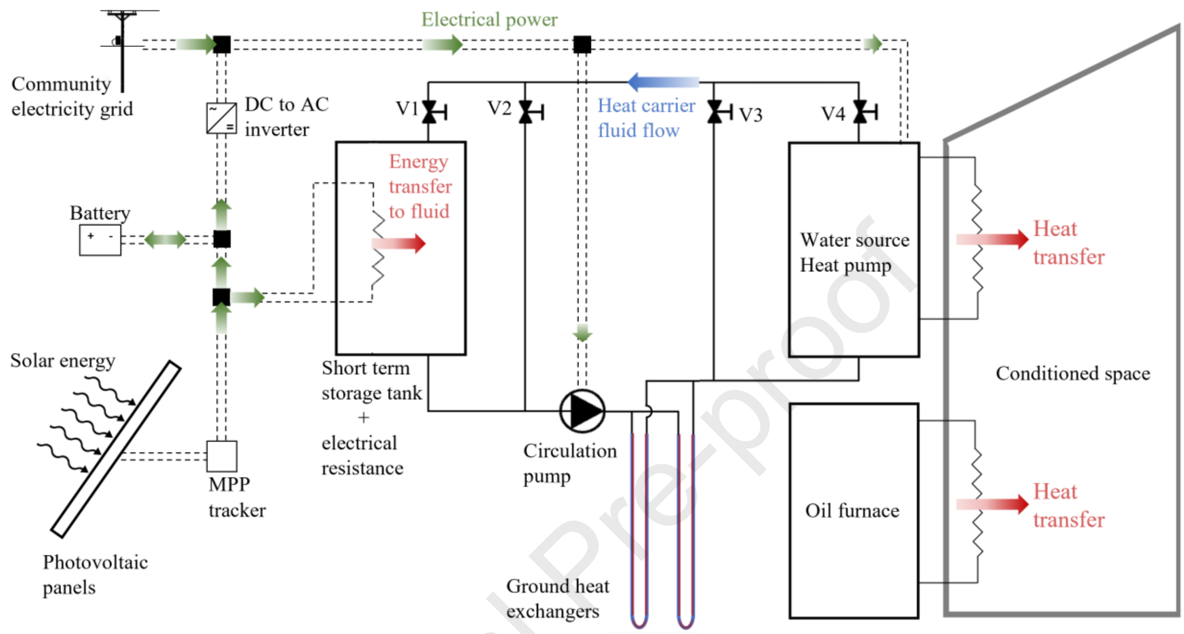

Fig. 3. Components of the SAGCHP and schematic configuration of the heating system under study.

The configuration of the SAGCHP allows four operation modes:

- Mode 0: In mode 0, the fluid does not circulate and no heat transfer between the components of the SAGCHP occurs (v2 and v3 opened, v1 and v4 closed). Nevertheless, heat exchanges between the ground volume around the borefield and its environment (the atmosphere and the surrounding ground) are possible. Mode 0 is used when the HP does not work and when the storage tank is unable to raise the exiting fluid temperature above a certain limit. Indeed, the circulation of the fluid is deemed undesirable when the pumping power exceeds the heat that could potentially be transferred from the storage tank to the ground. This usually happens when no heat from the HP is required, and when solar energy from the PV is unavailable or low.
- Mode 1: Mode 1 is required when the HP must provide heat to the house, and when the PV power production is sufficient to raise the temperature of the fluid coming from the HP. In that case, the fluid circulates in the storage tank before entering the GHE and the HP (v4 and v1 opened, v2 and v3 closed). Then, heat is transferred from the ground and from the storage tank to the HP.

- Mode 2: Mode 2 occurs when the HP does not work and when the PV production is sufficient to raise the temperature of the fluid exiting the storage tank. Indeed, the circulation of the fluid is deemed suitable if the heat transfer towards the ground exceeds the required pumping power. In that case, the fluid circulates in the storage tank and discharges heat into the GHE, helping to prevent its temperature depletion (v1 and v3 opened, v2 and v4 closed).
- Mode 3: Mode 3 replaces mode 1 when the storage tank is unable to raise the temperature of the fluid coming from the HP (v2 and v4 opened, v1 and v3 closed). Then, heat is only transferred from the ground to the HP.

A preliminary assessment of the expected fuel savings showed that using the local community grid to meet the entire electrical demand of the HP and the circulation pump is inappropriate for economic and environmental reasons. For example, let us assume a COP of 3 for the HP and a power plant efficiency of 34.1% [27]. Then, replacing one energy unit of fuel from the furnace requires 0.33 units of electricity at the HP compressor, i.e., 0.33/0.341 $\simeq$ 0.967 units of fuel at the power plant (i.e., virtually no reduction of the overall fuel consumption). It follows that the HP electricity consumption must at least rely partially on non-fossil fuel energy sources to limit the consumption of diesel associated with the electricity production. On the other hand, the small size of the community grid constitutes a limit to the amount of PV production that the grid can purchase when it exceeds the SAGCHP demand. In such context, the penetration of renewable energy sources is limited unless local means of storage are implemented. Thus, we compared two distinct scenarios of electrical supply to operate both HP and circulation pump: (i) directly from the PV/MPPT/inverter when the electricity production is coincident with the operation of the HP and the pump; (ii) from a battery in which the PV production can be stored. They are respectively called scenarios n/B and w/B. In the without battery (n/B), the match between the PV production and the HP and pump electrical demand constrained the electrical supply from the PV. The allocation of the electricity produced by the PV at a time t (i.e, $P_{\mathrm{PV}}(t)$) between the HP compressor, the pump and the storage tank was determined by:

$$P_{\mathrm{PV}\rightarrow\mathrm{HP}}(t) = MIN\left\{P_{\mathrm{PV}}(t)\ ;\ P_{\mathrm{elec,HP}}(t)\right\} \tag{1}$$

$$P_{\mathrm{PV}\rightarrow\mathrm{pump}}(t) = MIN\left\{P_{\mathrm{PV}}(t)\ ;\ P_{\mathrm{elec,HP}}(t) + P_{\mathrm{elec,pump}}(t)\right\} - P_{\mathrm{PV}\rightarrow\mathrm{HP}}(t) \tag{2}$$

$$P_{\mathrm{PV}\rightarrow\mathrm{tank}}(t) = P_{\mathrm{PV}}(t) - P_{\mathrm{PV}\rightarrow\mathrm{HP}}(t) - P_{\mathrm{PV}\rightarrow\mathrm{pump}}(t) \tag{3}$$

The scenario with battery (w/B) involves a battery to better match the PV production, the HP demand and the pump demand. The battery receives the electrical power from the PV until it is fully charged, and it provides electrical power to the HP and the pump until it is fully discharged. The storage tank receives the remaining PV production in the same manner as in n/B (see Eq. (3)). The pumping power was estimated based on the friction losses in the U-pipes of the GHE. In both scenarios, the community grid supplies the remaining electrical needs of the HP and the pump when the PV production cannot meet them entirely.

2.3 TRNSYS model description

The SAGCHP model was developed in TNRSYS and coupled with the building energy model described in Section 2.1. Table 1 summarizes the main parameters of the model. The heating thermostat provides the HP with a control signal (0 or 1) commanding its stopping and starting, depending on the instantaneous heating demand in the building. The model also includes PV panels (with an idealized MPPT) located on the roof of the building with the same inclination and orientation as in the house under study. Thus, the PV field is divided into two arrays with the same area and facing respectively the South and the North with a tilt angle of 18°. A part of the power produced by the PV is directly supplied to the storage tank model *type 4c* through its heating element, and the other part of the PV production directly supplies to the HP and the pump (scenario n/B) or the battery (scenario w/B). The HP was modeled with *type 919* (vapour-compression heat pump) and the PV, with *type 94* (crystalline modules). The borefield was modeled with *type 557a*. All simulations were run with a time step of ten minutes and for a duration of ten years. Shorter time steps of up to 2 minutes were tested and did not change the results significantly.

The sizing and modeling of the main components (i.e., HP, PV, boreholes and battery) is described below, along with the modeling of the control system. Again, specific values of the model parameters are shown in Table 1.

Heat pump: A water source HP with a rated heating capacity of 9.38 kW was chosen based on the heating demand of the building and available HP models. In this case, the HP can supply the whole building heating demand. Consequently, the furnace operating time reduces to nearly zero. The performance data from a manufacturer were used in *type 919*, accounting for variations of the COP and heating capacity as functions of entering temperature [28]. Fig. 4 provides the HP heating capacity and compressor power. The minimal inlet temperature of the HP is -6.5 °C.

PV array: A photovoltaic array with a rated power of 9 kW was selected based on the available roof surface area. The *type 94* models PV arrays with an idealized MPPT. The PV power output depends on the incident solar radiation and the ambient temperature according to the performance data from the manufacturer [29]. Table 1 provides the main data used in the PV model. Its nominal efficiency is 15.54%. We applied for all simulation years the solar radiation data of the year 2012 from [24] and assumed that snow did not accumulate on the arrays (in fact, the roof is designed in such a way that snow is constantly removed by wind).

Battery: In scenarios involving a battery, the latter was sized to ensure that electricity production of around two days could be stored. A capacity of 50 kWh was then chosen. Owing to the mismatch between the PV production and the HP consumption, this constitutes the maximum energy that could be produced and consumed when considering a two-day horizon for the storage strategy. It was found that increasing further the size of the battery did not improve significantly the performance of the system (diminishing return). A two-day horizon was deemed sufficient to smooth the supply and demand fluctuations. If the PV production exceeds the battery capacity, the electricity is converted in heat in the storage tank. We assumed an idealized battery with a charge and discharge efficiency of 100% and a depth of discharge of 100%. We also assumed an idealized DC-AC inverter (see Fig. 3).

Borefield: The borefield TRNSYS model assumes the ground properties to be uniform. As shown in Table 1, an average ground thermal conductivity of 2.35 W/(m.K) and an average ground thermal capacity of 2.25 MJ/(m^3.K) were chosen based on a report from Comeau et al. on the geothermal potential in Whapmagootui-Kuujjuarapik [30]. The average ground thermal properties considered in the present study are close to the pessimistic scenario 1A presented in their report for sand deposits over a granitic bedrock. The undisturbed temperature of the ground is 2.5 °C [30]. Assuming that the boreholes would be mostly located in the bedrock, which has a very low water content, the freezing and thawing of water in the borefield was not modeled. Owning to the geothermal potential in Whapmagoostui and to the building heat load, a total GHE length of approximately 260 m was found to be sufficient to ensure that the temperature of the fluid at the HP inlet is always above −6.5 °C [30]. Underground thermal storage systems usually involve several shallow boreholes, closely placed and in strong thermal interaction with each other. However, in the present case and as will be detailed below, the PV production is insufficient to totally balance the yearly ground heat extraction and perform underground thermal storage. Thus, the borefield includes two 130 m-deep boreholes to insure sufficient heat transfer between the surrounding ground and the ground volume in the borefield. They are connected in series and are spaced by 6 m. The fluid mixture (35% water-propylene-glycol mixture) prevents the freezing of the heat transfer fluid in the pipes (freezing temperature of -16 °C) [31]. The GHE model (*type 557a*) requires two temperature boundary conditions at the surface: one at the surface above the borefield and another one at the ground surface around the borefield. The snow cover creates an insulation layer between the ground and the atmosphere for several months, preventing the ground surface temperature from following the atmosphere temperature [32]. In order to estimate the appropriate surface boundary conditions via heat balances, the following assumptions were made: the thermal inertia of the snow cover is neglected; the variation of the mean borefield temperature from a time step to another is small enough to consider its value at the previous time step to perform the surface heat balance; the temperature in the higher part of the borefield is close to the mean borefield temperature; and the temperature of the ground in the surroundings of the borefield is close to the undisturbed ground temperature. Performing an energy balance and isolating the surface temperature yields, at each time step:

$$T_{s1}(t) = \frac{\frac{k_g}{H_{header}} T_{borefield}\left(t - \frac{1}{6}\right) + UT_a(t)}{\frac{k_g}{H_{header}} + U} \quad \text{(top borefield)} \tag{4}$$

$$T_{s2}(t) = \frac{\frac{k_g}{H_{header}} T_g + UT_a(t)}{\frac{k_g}{H_{header}} + U} \quad \text{(top surroundings)} \tag{5}$$

where T_g is the undisturbed ground temperature (constant over time), $T_{borefield}$, the average temperature of the ground volume included in the borefield, T_a, the air temperature, H_{header}, the depth of the top of the heat exchangers, and k_g, the ground conductivity (see Fig. 5). The volume of ground included in the borefield is 8,105 m^3. U is the overall heat transfer coefficient of the layers located between the ground surface and the atmosphere. Two values were used: one in the presence of a snow cover, and one without it. These two values were calibrated to meet the following conditions:

- The yearly average surface temperature must be equal to the undisturbed ground temperature (2.5 °C) when no perturbation of the ground occurs (no heat extraction nor injection).
- When a snow cover is present (i.e., from day 1 to 135, and from day 307 to 365), the surface temperature stabilizes to −1 °C, according to ground temperature data collected at Whapmagoostui [25], and the heat transfer is dominated by conduction in the snow.
- According to this same dataset, the undisturbed ground surface temperature closely follows the air temperature once the snow cover has disappeared (heat transfer dominated by convection and radiation).

In the end, U was set to 0.56 W/(m^2.K) during the snow cover period or whenever the air temperature was below –0.5 °C. Otherwise, U was set to 20 W/(m^2.K). These empirical values allowed matching the ground temperature data.

Table 1. Values of the main parameters in the model.

TRNSYS component	Parameter	Units	Value
GHE – *type 557a*	Borehole depth	m	130
	Boreholes spacing	m	6
	Undisturbed ground temperature [30]	°C	2.5
	Borehole radius [33]	m	0.0762
	Backfill thermal conductivity [30]	W/(m.K)	1.5
	Pipe outer radius [34]	m	0.024
	Pipe inner radius [33], [34]	m	0.019
	Pipe thermal conductivity (HDPE pipe)	W/(m.K)	0.4
	Half shank spacing	m	0.025
	Header depth	m	2
	Ground thermal conductivity [30]	W/(m.K)	2.35
	Ground heat capacity [30]	MJ/(m^3.K)	2.25
HP – *type 919*	Rated air flowrate	L/s	542
	Rated liquid flowrate	m^3/h	2.6
	Rated heating capacity	W	9,380
	Rated COP	-	3.5
Storage tank – *type 4c*	Volume [34]	m^3	0.8
	Loss coefficient [34]	W/(m^2.K)	0.33
	Number of temperature nodes	-	50
PV array – *type 94* (all parameters from [29])	Number of modules in series	-	6
	Number of modules in parallel	-	3
	Module area	m^2	1.48
	Module maximum power	W	250
	Nominal module efficiency	%	15.54
	Array slope	degrees	18
	Short-circuit current at reference conditions (I_{sc})	A	8.87
	Open-circuit voltage at reference conditions (V_{oc})	V	37.2
	Current at MPP and reference conditions	A	8.3
	Voltage at MPP and reference conditions	V	30.1
	Temperature coefficient of I_{sc}	A/K	0.0058
	Temperature coefficient of V_{oc}	V/K	-0.1265
	Number of cells wired in series	-	60
	Optimum operating current (I_{mp})	A	6.60
	Optimum operating voltage (V_{mp})	V	27.5

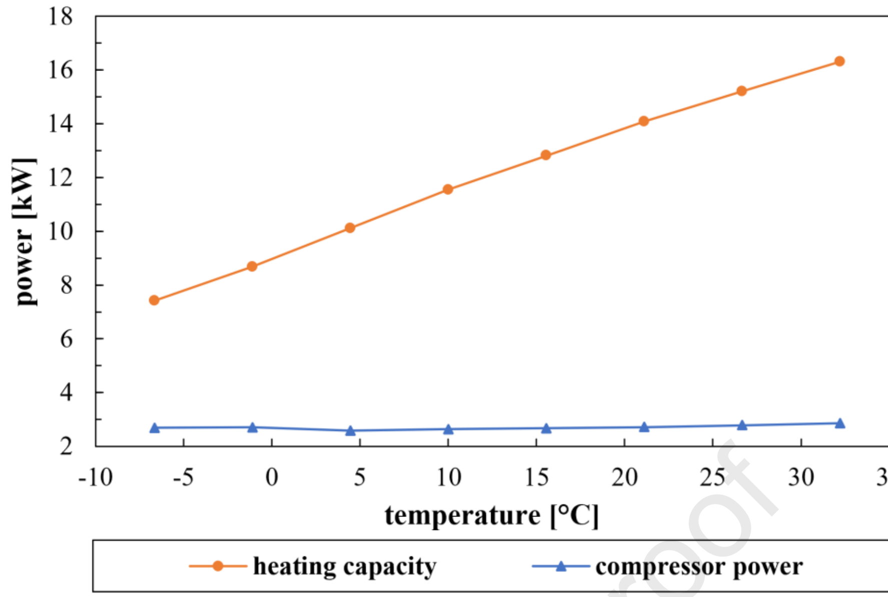

Fig. 4. Heat pump heating capacity and compressor power depending on the entering fluid temperature.

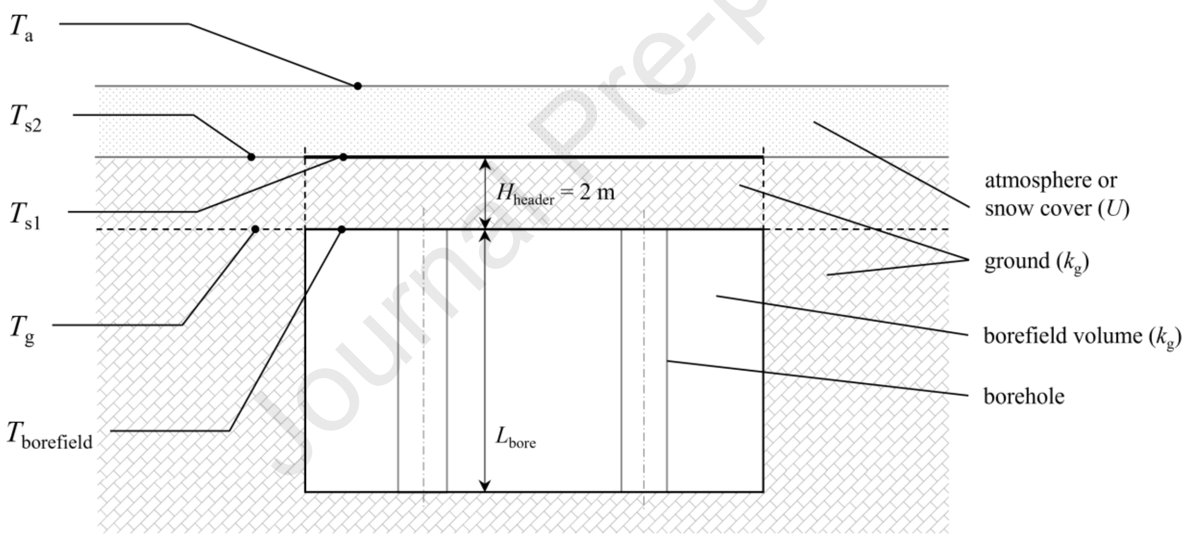

Fig. 5. Schematic representation of the ground volume including the boreholes, and its surroundings.

Control: The algorithm to change the operation mode during the simulation is schematized in Fig. 6. It constitutes the application of the principles described in Section 2.2. Signal values govern the opening and closing of the flow diverters in the TRNSYS model. At each simulation time step, the calculation of governing signals is based on the fluid temperature at the previous time step. For selecting Mode 2, a condition has been added to limit the electricity consumption associated with the fluid circulation in the SAGCHP. First, we calculate the pumping power required to move the fluid in the ground heat exchangers. Only friction losses in the U-pipes were considered. The amount of heat that can be injected into the ground is also calculated from:

$$P_{\mathrm{GHE}}(t) = \left(\dot{m}C_{\mathrm{p}}\right)_{\mathrm{f}}\left(T_{\mathrm{out,tank}}\left(t-\frac{1}{6}\right)-T_{\mathrm{out,GHE}}\left(t-\frac{1}{6}\right)\right) \quad (6)$$

When Mode 2 is used in the previous time step, it is kept for the next time step if the heat transfer rate defined by Eq. (6) is larger than the pumping power. Otherwise, the circulation is stopped (Mode 0). When Mode 0 was used at the previous time step, Mode 2 was only triggered when the storage tank temperature was 0.5 °C warmer than the minimal value ensuring a P_{GHE} value higher than the pumping power. This was implemented to limit excessive changes of states between Modes 2 and 0.

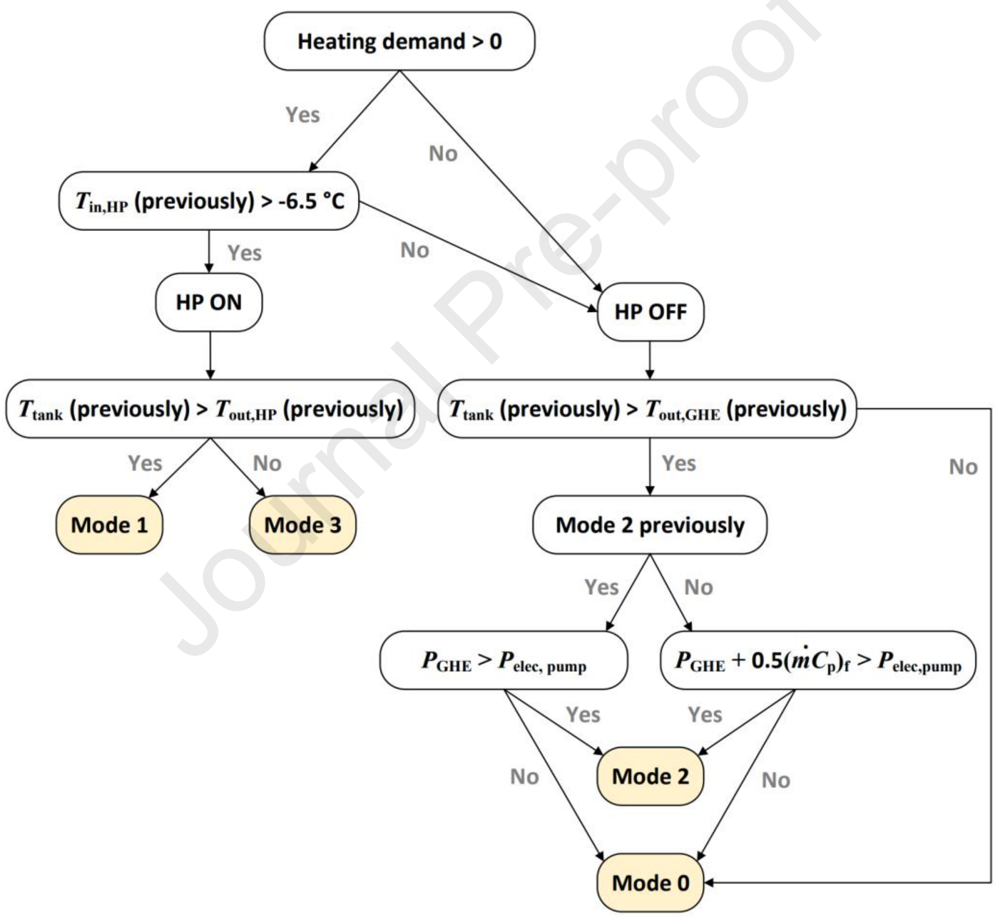

Fig. 6. Algorithm ruling changes of operation modes during the simulation.

3. Simulation results for scenarios with and without battery

This section describes the behavior of the SAGCHP system. Fig. 7 reports the long-term evolution of the fluid temperature in the SAGCHP and the mean temperature of the ground volume around the boreholes (mean borefield temperature), during a ten-year operation, for both scenarios n/B and w/B.

Even though simulations were carried out with a ten-minute time step, only daily averages are reported in the figure for the sake of clarity. When calculating the daily average of $T_{\text{in,GHE}}$ and $T_{\text{out,GHE}}$, only time steps in which the system operated in modes 1, 2 or 3 were accounted for. Similarly, only modes 1 and 3 (i.e. when the fluid circulated in the HP) were considered for the calculation of the daily average of $T_{\text{in,HP}}$ and $T_{\text{out,HP}}$. It should be noted that the fluid temperature exiting the GHE corresponds to the fluid temperature entering the HP only during operation modes 1 and 3. The daily average of $T_{\text{out,GHE}}$ also includes the heat injection periods during operation mode 2. Thus, its value is higher than $T_{\text{in,HP}}$. The evolution of the fluid and ground temperatures is influenced mainly by the PV production, the space-heating demand from the building and the outdoor temperature conditions, which explains the shape of the curves in Fig. 6. The fluid temperature entering the HP ($T_{\text{in,HP}}$) is always above the limit imposed by the HP (i.e., above -6.5 °C), preventing the HP from stopping. Finally, a long-term thermal depletion of the ground occurs over the ten-year operation. The borefield temperature (see definition below Eq. (5)) falls from 2.5 °C at the beginning of the simulation, to respectively 0.87 °C and 0.54 °C at the end of the simulation for both scenarios without (n/B) and with battery (w/B). The evolution of the HP COP depends on the entering HP fluid temperature and thus, follows the same trend: in the scenario without battery (n/B), its annual average falls from 3.25 for the first simulation year to 3.18 for the last simulation year, while it falls from 3.22 to 3.14 in the scenario with battery (w/B).

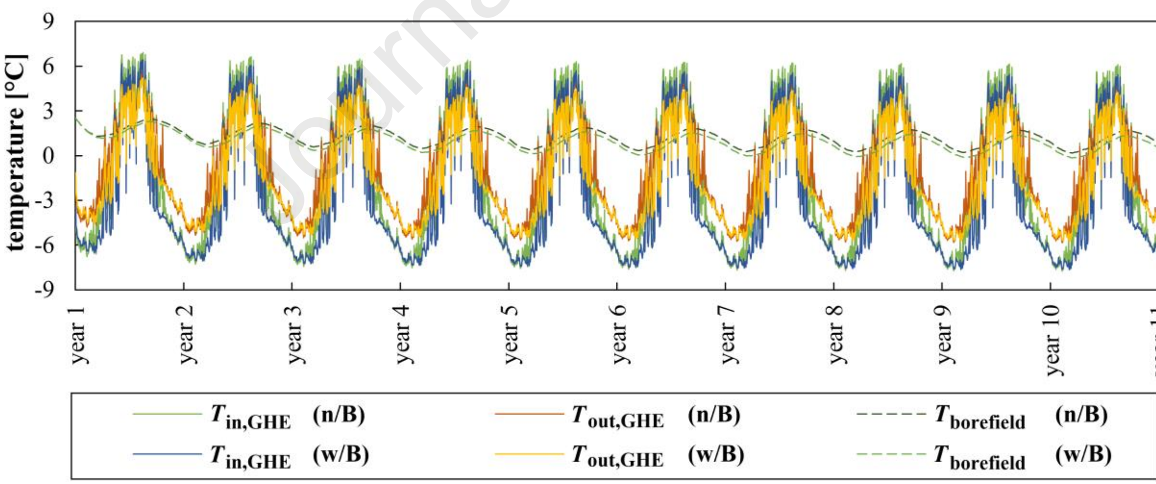

(a)

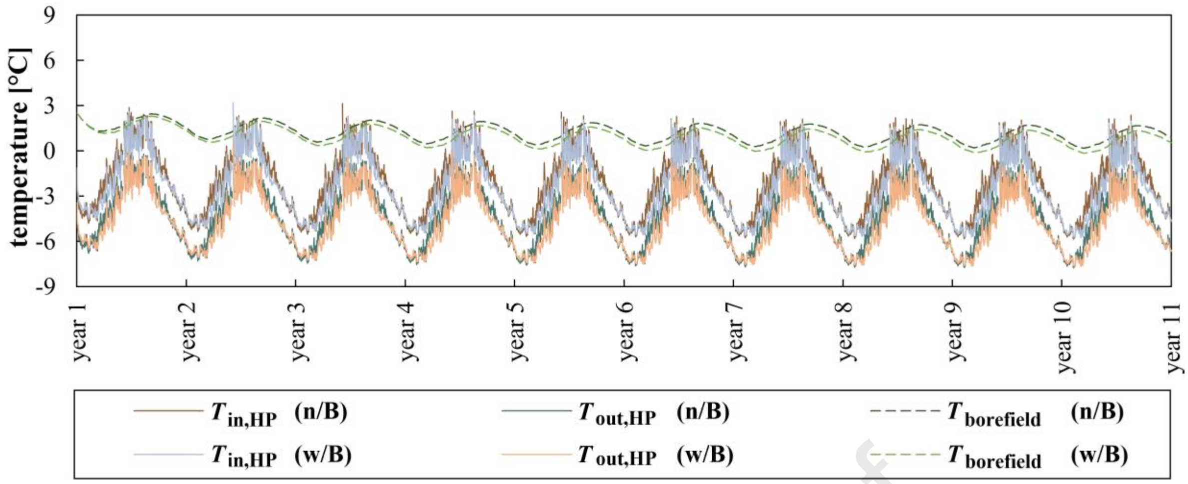

(b)

Fig. 7. (a) Daily average of fluid temperature entering and exiting the GHE, and of mean borefield temperature over ten years of operation for scenarios n/B and w/B, **(b)** Daily average of fluid temperature entering and exiting the HP, and of mean borefield temperature over ten years of operation for scenarios n/B and w/B.

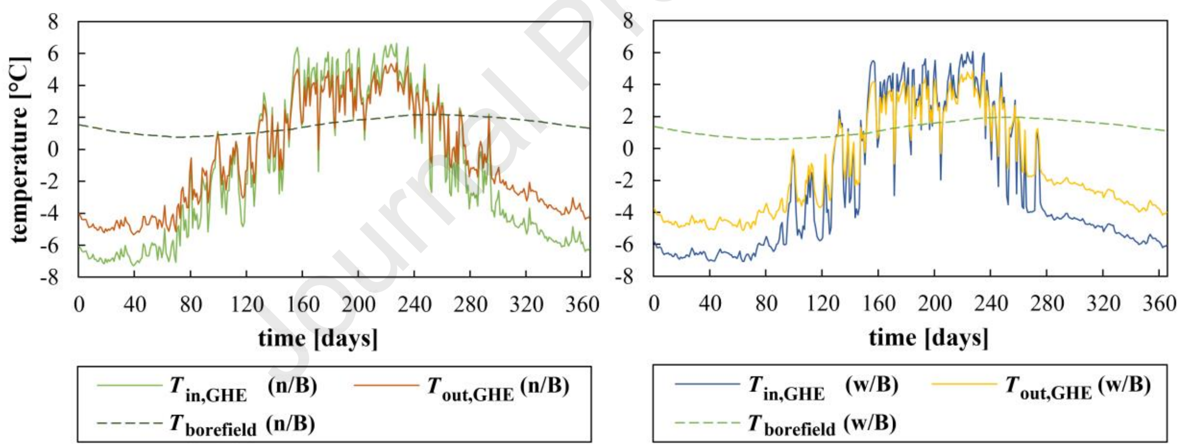

(a) **(b)**

Fig. 8. Daily average fluid temperature entering and exiting the GHE during the second year of operation, for scenario n/B **(a)** and for scenario w/B **(b)**.

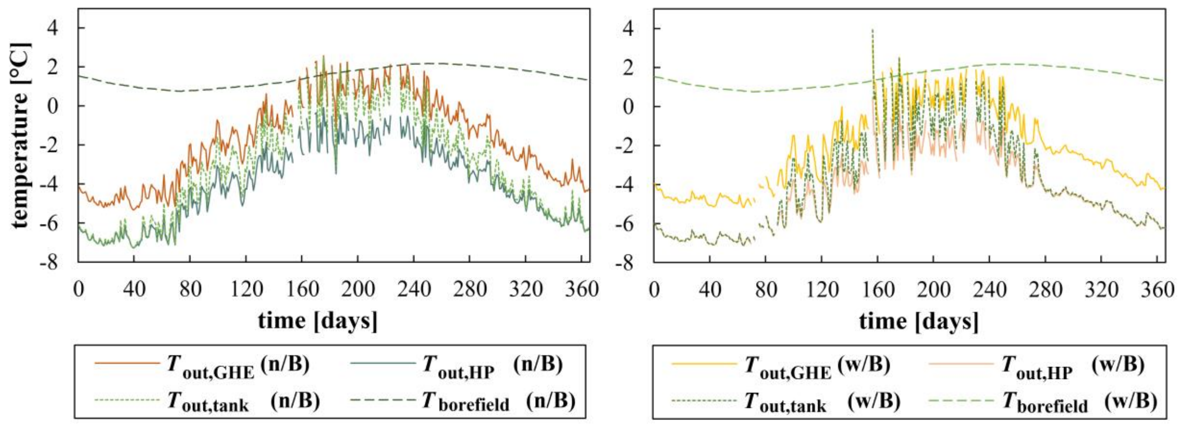

(a) (b)

Fig. 9. Daily average fluid temperature exiting the tank, the GHE and the HP during operation mode 1, during the second operation year, for scenarios n/B **(a)** and w/B **(b)**.

Fig. 8 offers a zoom of the daily average fluid temperature entering and leaving the GHE during operation modes 1, 2, 3, and the borefield temperature during the second year of operation, for both scenarios n/B and w/B. That year was chosen to limit the impact of the initial conditions, but as was seen before, results are similar from one year to another. Fig. 8 highlights the change of direction of the heat transfer rate between the ground and the fluid over the year. $T_{out,GHE}$ exceeds $T_{in,GHE}$ when the heat transfer rate extracted by the HP overcomes the heat transfer rate injected in the ground by the solar assistance system (extraction mode). The contrary occurs in the middle of the year when a large quantity of solar energy is available (recharging mode). By comparing Figs. 8a and 8b, it is also visible that the fluid temperature oscillations are more pronounced in n/B during the extraction mode. Although the solar assistance allows slightly increasing the mean fluid temperature in the GHE and the HP during the extraction mode, it produces little change in the general temperature profiles for the second operation year. The discrepancies between n/B and w/B for the borefield temperature are more pronounced after ten years, as shown on Figs. 7a and 7b. Fig. 9 reports the fluid temperature exiting the storage tank, the GHE and the HP during operation mode 1. The differences between these three temperatures are directly related to the direction of the heat flows in the SAGCHP components. The differences ($T_{out,HP}$ – $T_{out,GHE}$), ($T_{out,tank}$ – $T_{out,HP}$) and ($T_{out,GHE}$ – $T_{out,tank}$) are proportional respectively to the heat transfer rate from the fluid to the HP, the amount of heat transferred to the fluid by the storage tank, and the amount of heat transferred from the ground to the fluid. It must be noted that the difference ($T_{out,tank}$ – $T_{out,HP}$) is positive or null most of the time, highlighting the fact that the storage tank preheats the fluid exiting the HP before entering the GHE when solar energy is available. Fig. 10 explicitly shows the direction of these heat flows in the SAGCHP, but takes into account all operation modes (i.e., 0, 1, 2, and 3), whereas Fig. 9 only shows mode 1. It can be seen that the average heat transferred to the HP follows the same trend as the daily average building heat demand. In agreement with previous results, Fig. 10 highlights the injection of heat in the ground when the power available from the solar assistance overcomes the heat extracted by the HP. On the contrary, when solar energy is less available in winter, the power extracted by the HP comes from the ground essentially. Figs. 9 and 10 also show the discrepancies in the heat provided by the tank between scenarios n/B and w/B. They are mostly visible before the 120th day and after the 240th day of the year, when the HP and pump electricity needs exceed the PV production. In fact, the use of a battery in scenario w/B does not change the amount of heat injected in the ground in the middle of the year but prevents the contribution of the storage tank during the coldest days.

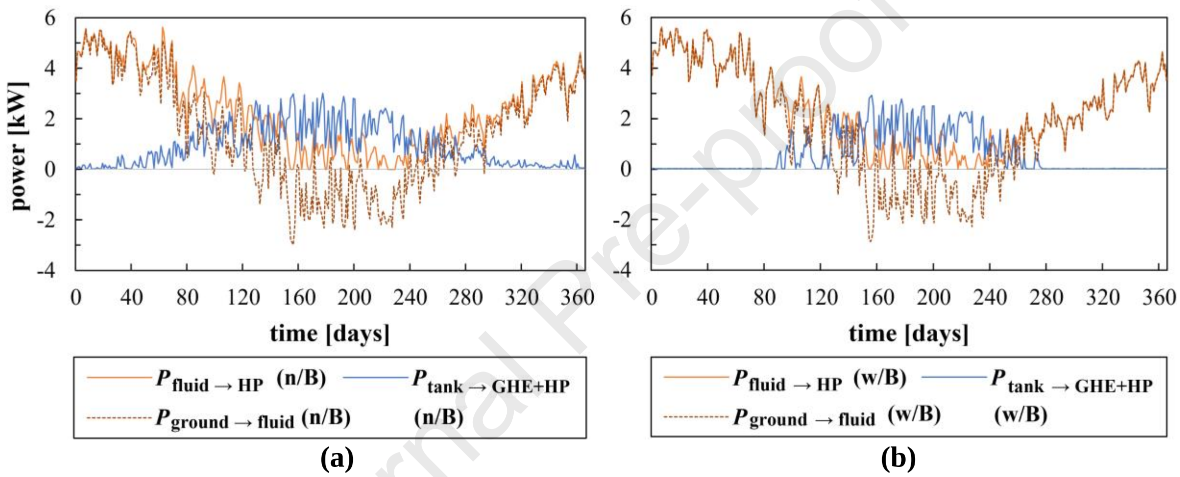

Fig. 10. Daily average of the heat transfer from the storage tank to the fluid, from the ground to the fluid, and from the fluid to the HP, during operations modes 0, 1, 2, 3, during the second operation year, for scenario n/B **(a)** and for scenario w/B **(b)**.

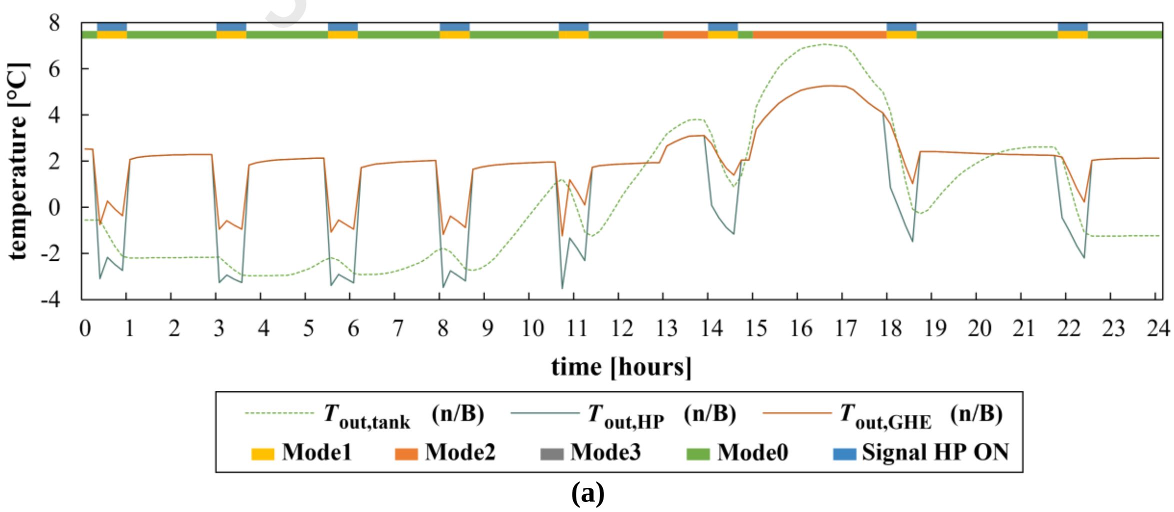

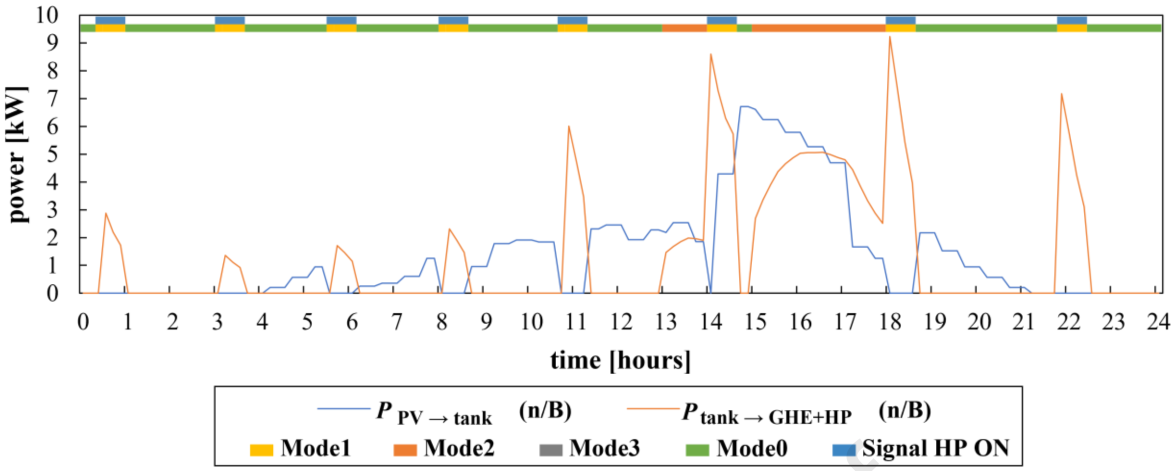

(b)

Fig. 11. (a) Temperature of the fluid exiting the tank, the GHE and the HP, and HP control signal, **(b)** Heat transfer rate from the PV to the tank and from the tank to the fluid, during the 182nd day of the second operation year in scenario n/B.

Fig. 11 helps to understand the alternance of the operation modes, by looking at results with a smaller time granularity. Only scenario n/B was considered as no significant differences were observed in scenario w/B regarding how the operation modes are used. One specific day was chosen to illustrate how the system is controlled (day 182, i.e., in summer). All ten-minute time steps are represented in the figures. Operation modes 1 and 3 occur when the HP operates (signal HP ON ≠ 0 in Fig. 11). More specifically, operation mode 1 occurs when the temperature of the fluid exiting the storage tank exceeds the temperature of the fluid exiting the HP, and operation mode 3, when it does not. Operation mode 2 occurs when no heating from the HP is required (signal HP ON = 0 in Fig. 11), and when the temperature of the fluid exiting the storage tank sufficiently exceeds the temperature of the fluid exiting the GHE. Mode 0 occurs when it does not. Fig. 11b reports the power supplied by the PV to the storage tank and the heat transfer rates from the storage tank to the other SAGCHP components. The figure shows that the heat transfer from the storage tank to the components occurs during operation modes 1 and 2, and that this heat is transferred to the ground, or to the HP, or to both components, depending on the relative position of the three curves in Fig. 11a. For instance, for operation mode 1, when $T_{out,tank} > T_{out,GHE} > T_{out,HP}$, it means that heat is transferred from the storage tank towards the ground and the HP, and when $T_{out,GHE} > T_{out,tank} > T_{out,HP}$, it means that that heat is transferred from the ground and from the storage tank to the HP. More generally, Fig. 11 confirms that the ability of the storage tank to provide heat to the system (the ground or the HP) depends strongly on the solar energy availability, which fluctuates during the day.

4. Impact of battery on the operation and performance

In this section, we analyze in more detail the impact of the battery on the performance of the system. Fig. 12 reports the distribution of the electric power produced by the PV delivered to the short-term storage tank, the HP and the pump in scenarios n/B and w/B, throughout the second operation year. In both cases, the photovoltaic power production is the same (P_{PV}). However, the way in which the electricity is used is different. In scenario n/B (Fig. 12a), the share of electricity used as heat is higher than in scenario w/B (Fig. 12b), because the use of a battery allows better matching the HP demand to the PV production. The battery allows the HP compressor to operate with the electricity from the PV (which is highly beneficial to reduce the recourse to fossil fuel), even when no instantaneous solar radiation might be available. Thus, the share allocated to the battery and ultimately to the HP and the pump in scenario w/B is greater than the share directly allocated to the HP and the pump in scenario n/B.

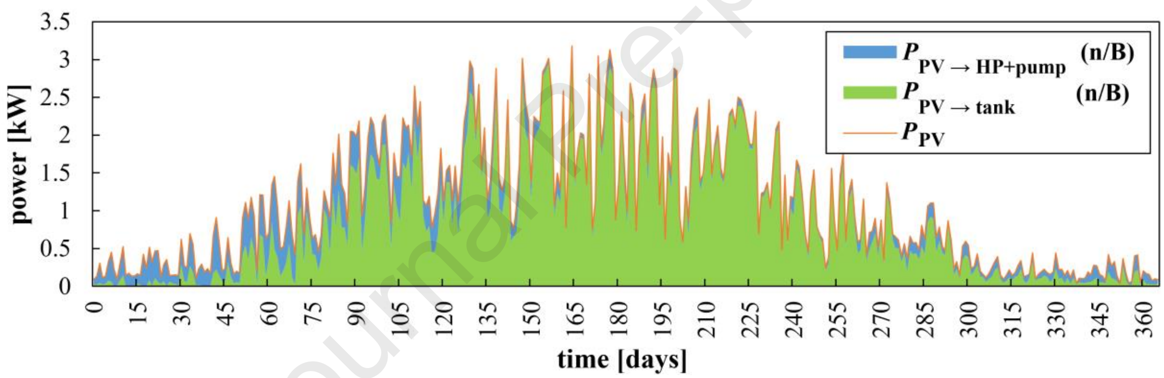

(a)

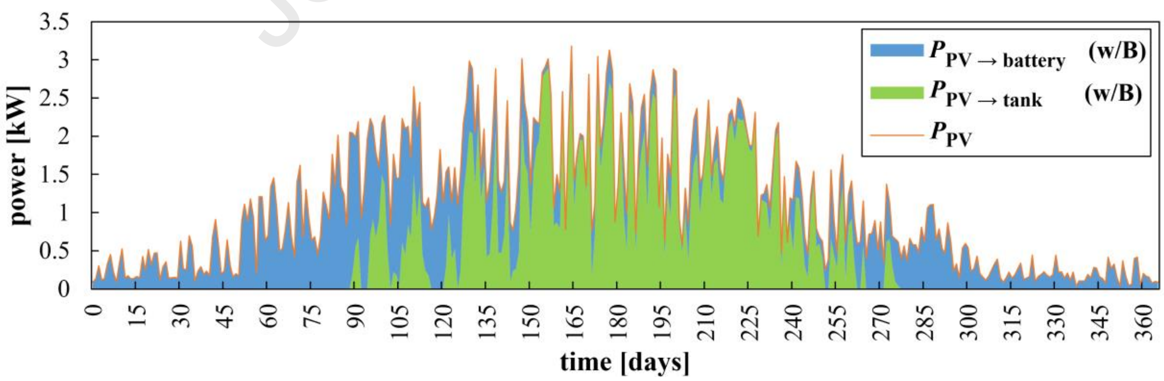

(b)

Fig. 12. End-use breakdown of how the average daily electricity produced by the PV is used **(a)** without battery, and **(b)** with battery.

Fig. 13 illustrates the match between the HP demand and the power supplied by the battery over the course of the year, in scenario w/B. For the sake of clarity, the electrical pump demand was not represented, as its impact battery state of charge is insignificant. The figure reports the daily average value of the electrical power required at the HP compressor, as well as the electric power supplied by the PV to the battery and by the battery to the HP. The community power grid is assumed to supply the remaining required electricity to the HP compressor (i.e., the difference between $P_{\mathrm{elec,\ HP}}$ and $P_{\mathrm{battery}\rightarrow\mathrm{HP}}$). A mismatch between the PV production and the HP electrical consumption occurs in winter months, from day 1 to 75 and from day 300 to 365. Unfortunately, this induces an additional electrical load to the community grid at the same time. It can be seen in Figs. 13a, b, and c that, most of the time, the curves $P_{\mathrm{PV}\rightarrow\mathrm{battery}}$ and $P_{\mathrm{battery}\rightarrow\mathrm{HP}}$ remain very close, indicating that the battery acts mainly as a short-term energy storage facilitating the match between the electricity production (when daylight is available) and its use (the rest of the day or in the next few days). That being said, there is also a slow charging of the battery during the summer and a slow discharging during winter, and the battery state of charge exceeds 85% for nearly 152 days of the year.

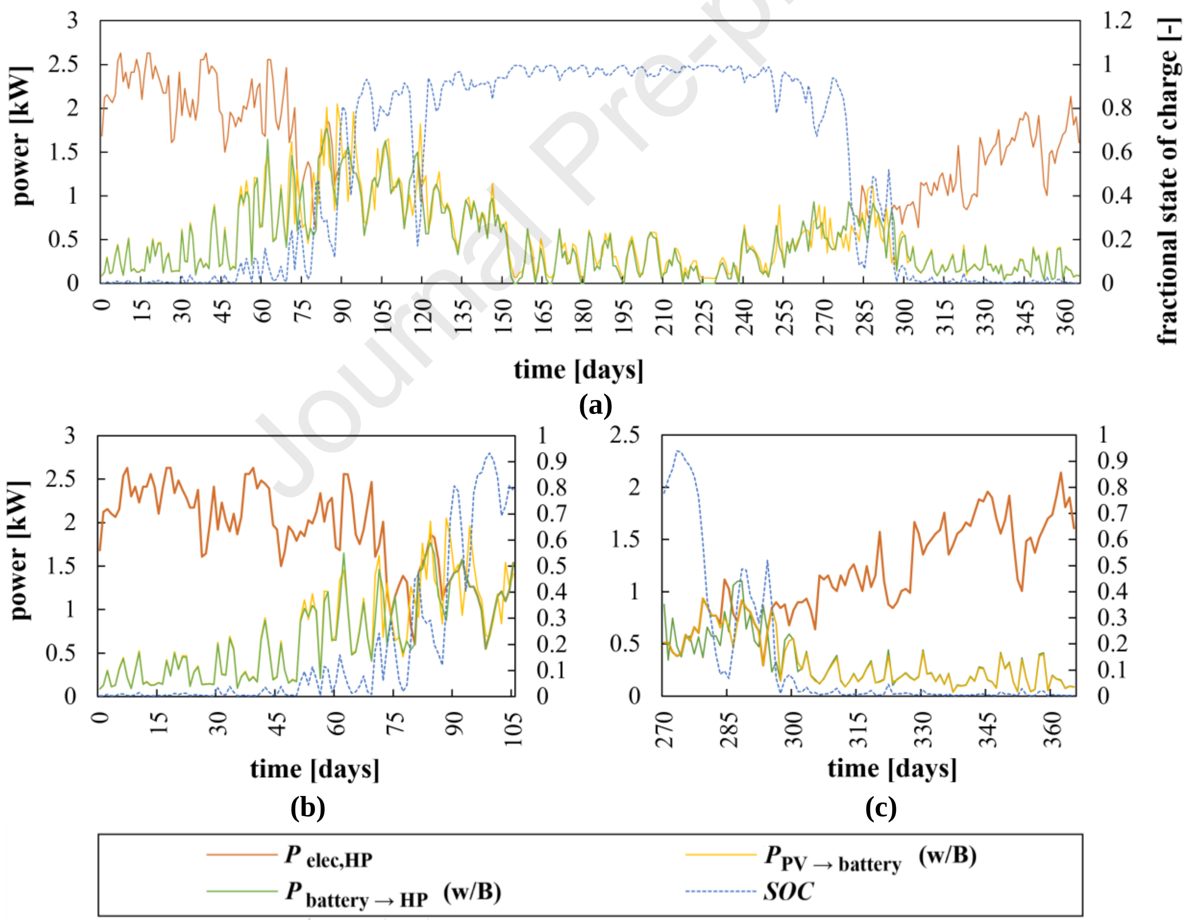

Fig. 13. Daily average value of the power needed by the HP compressor, the power supplied by the PV to the battery, the power transferred from the battery to the HP, and the battery fractional state of charge during the second operation year from day 1 to 365 **(a)**, from day 1 to 105 **(b)** and from day 270 to 365 **(c)**, for scenario w/B.

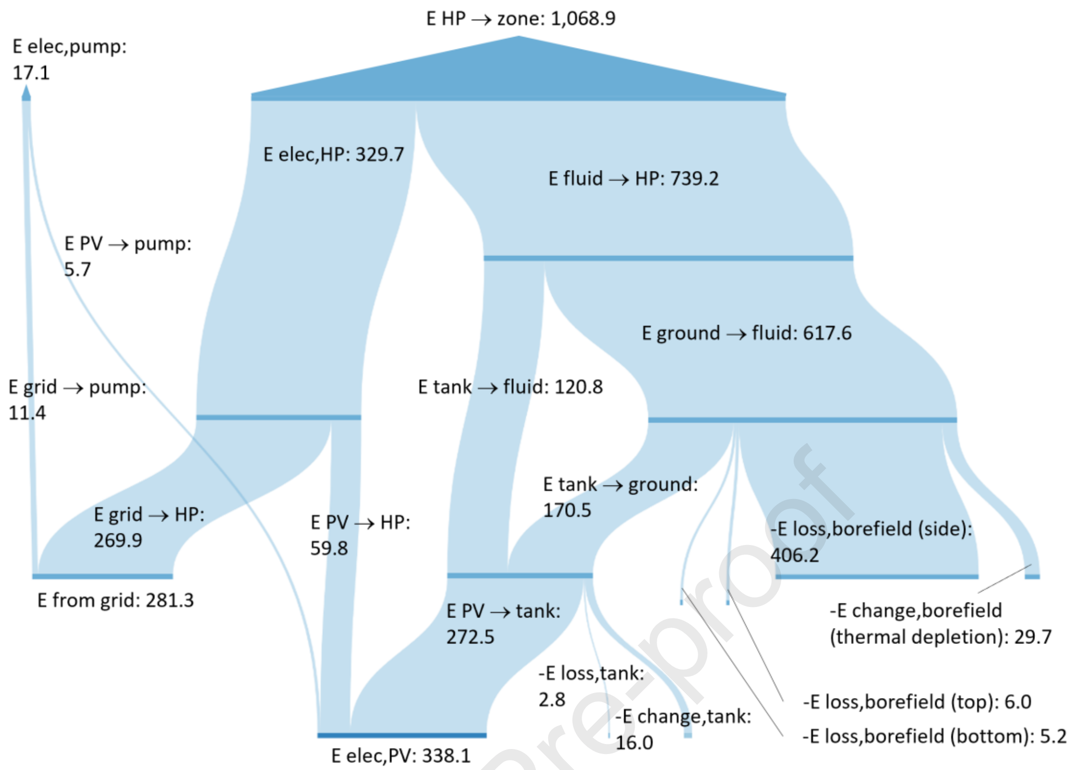

(a)

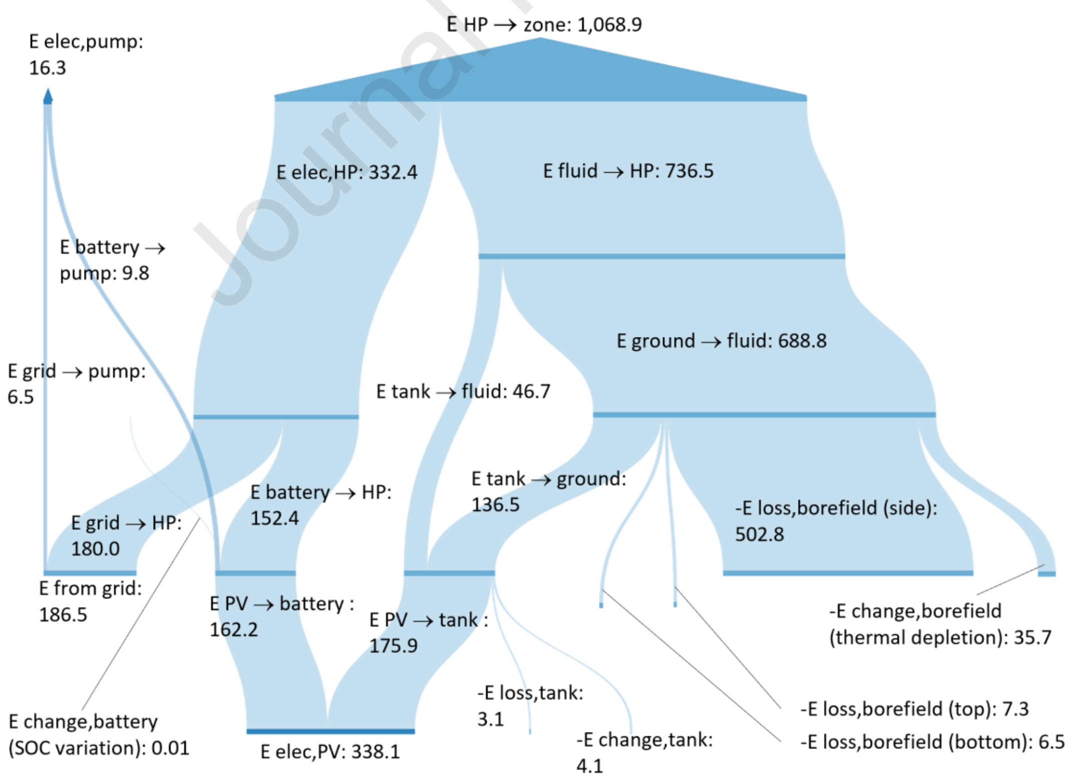

(b)

Fig. 14. Sankey diagram of the energy balance of the SAGCHP for a ten-year operation, in GJ, **(a)** for scenario n/B and **(b)** for scenario w/B.

Fig. 14 summarizes the total energy balance of the SAGCHP with and without a battery, over ten years of operation. As shown previously, the PV production allocated to the HP and the pump ultimately increases with a battery. Adding a battery to the system increases by 147.6% the electricity provided by the PV to the HP and the pump, and consequently, decreases by 37.1% the energy transferred from the short-term storage tank to the fluid. A part of this heat is directly supplied to the HP without being stored in the ground ($E_{\text{tank}\rightarrow\text{fluid}}$), while the other part contributes to the ground energy balance ($E_{\text{tank}\rightarrow\text{ground}}$). In scenario n/B, 41.5% of this heat is directly supplied to the HP while the remaining 58.5% is injected in the ground (Fig. 14a). In scenario w/B both percentages reach 25.5% and 74.5% (Fig. 14b). With the battery, the amount of heat extracted from the ground (the borefield and the surrounding ground) increases by 23.6%, the amount of heat transferred from the environment (the surrounding ground and the atmosphere) to the borefield increases by 23.8%, and the resulting borefield thermal depletion increases by 20.2%. The total HP electricity needs increase by 0.8% with the battery due to a small reduction of the COP caused by the ground thermal depletion. When taking into account all the effects of the battery on the HP efficiency and on the HP electricity supply, the total amount of required energy from the community grid decreases by 33.7%, dropping from 281.3 GJ in scenario n/B to 186.5 GJ in scenario w/B.

5. Fuel saving assessment

The fuel saving (with respect to the reference scenario, i.e. with only a fuel oil furnace) resulting from the use of the SAGCHP for ten years can be easily estimated with:

$$FS = \left[\frac{E_{\text{HP}\rightarrow\text{zone}}}{\eta_{\text{furnace}}} - \frac{E_{\text{grid}\rightarrow\text{HP+pump}}}{\eta_{\text{power plant}}} \right] \frac{1}{LHV} \tag{7}$$

where $E_{\text{HP}\rightarrow\text{zone}}$ is the amount of heat provided by the heat pump system to the building, $E_{\text{grid}\rightarrow\text{HP+pump}}$ is the electricity provided by the community grid. Around 4% of this energy is allocated to the pump in both scenarios n/B and w/B. The calculation of the saving also involves the efficiency of the fuel oil furnace and that of the power plant (respectively 80% and 34.1%), as well as the heating value of the fuel, which was assumed to be 36.0 MJ/L [35]. The scenario without a battery (n/B) allows a total fuel saving of 14,195 L and that with the battery (w/B), of 21,924 L, over ten years. Scenarios n/B and w/B respectively induce an increase of 22,917 L and 15,190 L of the diesel community power plant consumption, while they both allow saving around 37,112 L at the house furnace. These values can be compared to the current consumption, i.e., when only a fuel oil furnace is used, which is 37,120 L. This latter value is obtained by dividing the space heating need by the furnace efficiency and the diesel lower heating value. This means that the systems without a battery and with a battery allow reducing the fuel consumption by 38.2% and 59.1%, respectively. Decreasing the electricity consumption allows substantial fuel savings owning to the low diesel plant efficiency (34.1%), in comparison with the fuel savings performed with the substitution of more efficient fuel oil furnaces (80% efficiency).

6. Discussion on limitations and future work

As shown in this work, SAGCHP systems present a potential energy solution for isolated and remote communities, but adapted economic, design procedures and demonstration projects are still needed to be able to deploy them in the future. Future work could also investigate the performance of larger SAGCHP that could service a group of houses (e.g., district heating) in remote communities. This could help to limit initial costs and facilitate the maintenance of the system as local workforce is limited [36], [37]. It would also be relevant to simulate the SAGCHP in other villages. Whapmagoostui is located in the South of the Nunavik region, and it would be interesting to verify how the conclusions of the present work are influenced by even more extreme weather conditions at higher latitudes where the undisturbed ground temperature is below 0°C. The influence of year-to-year weather variabilities on the system performance also needs to be investigated, in particular to establish whether it amplifies the ground thermal imbalance. The influence of global warming on the ground undisturbed temperature and system performance could also be investigated. It would be of great interest to assess the risk of snow accumulation on the PV as it could reduce their production and the system performance. The issue of winter electricity demand also needs to be addressed. In this regard, wind energy could play a greater role as wind turbines are expected to be implemented in the coming years in the communities of Whapmagoostui-Kuujjuarapik [38], [39]. The SAGCHP system could be simulated in other geological environments (e.g., unconsolidated sediments or environments with underground water flow and groundwater phase change) as this could influence the thermal behavior of the borefield and shift the HP performance [8], [40], [41]. Finally, several simplifying assumptions were made in this work and could be further relaxed in future work. Studying in more details the interactions between the PV arrays, the Maximum Power Point Tracker, the battery, the DC/AC inverter, and the community grid could be relevant, as this could add constraints to the electricity supply model. The features of the system (e.g. array size, battery size, number of boreholes, etc.) could also be further optimized [42].

7. Conclusions

The goal of the present work was to model a photovoltaic SAGCHP supplying space heating to a Nunavik house and to assess its long-term performance over ten years. An energy model of a house located in the isolated community of Whapmagoostui (Nunavik, Quebec, Canada) was developed and validated from energy bills. Then, a SAGCHP model was elaborated accounting for its different operation modes. The system is connected to the community electricity grid and includes a 9.38-kW heat pump, 9-kW PV arrays, an 800 liters water tank and two 130 m-deep borehole heat exchangers. Simulations were carried out with and without a battery. In all cases, a part of the PV production was used by the heat pump compressor and the circulation pump, either instantly (case without battery) or via the battery. The rest of the PV production was used as heat (stored in the ground or used directly at the heat pump).

Without a battery, we found a ground temperature depletion of 1.6 °C during the ten-year operation, and with a battery, the depletion was 2.0 °C. Using an electrical battery allows decreasing the part of the heat pump electricity demand supplied by the community grid. Using photovoltaic production for the SAGCHP electricity supply has more impact on the global fuel consumption than its use for heat supply and seasonal storage purposes, as the latter improves negligibly the HP efficiency. SAGCHP allows reducing fuel consumption by 38.2% (system without battery) and 59.1% (system with battery). However, the solar assistance failed to avoid additional electrical load on the community grid induced by the system operation in winter.

To date, several studies have assessed the geothermal potential and the economic viability of GCHP in Nunavik mostly focusing on the ground heat transfer aspects (see, for example, Refs. [5] to [9] introduced in the introduction). However, the present paper provides a new perspective by exploring more thoroughly the interactions between heat exchanges in the ground, electrical energy production and storage, and the behavior of the different components of the system during each simulation time step of a ten-year operation. This constitutes a necessary step before future work can address the economic aspects, the optimization of the system or investigate other configurations and technologies.

Acknowledgements

This work was financially supported by the *Institut nordique du Québec*, *Sentinelle Nord* and the New Frontiers in Research Fund.

References

[1] J. Royer, 'Status of Remote/Off-Grid Communities in Canada', Government of Canada, Jun. 2013. Accessed: Dec. 02, 2021. [Online]. Available: https://www.nrcan.gc.ca/energy/publications/sciences-technology/renewable/smart-grid/11916

[2] K. Karanasios and P. Parker, ‘Recent Developments in Renewable Energy in Remote Aboriginal Communities, Quebec, Canada’, *Papers in Canadian Economic Development*, vol. 16, pp. 98–108, 2016, doi: doi.org/10.15353/pced.v16i0.
[3] E. Gunawan, N. Giordano, P. Jensson, J. Newson, and J. Raymond, ‘Alternative heating systems for northern remote communities: Techno-economic analysis of ground-coupled heat pumps in Kuujjuaq, Nunavik, Canada’, *Renewable Energy*, vol. 147, pp. 1540–1553, Mar. 2020, doi: 10.1016/j.renene.2019.09.039.
[4] ‘Rise in the cost of gasoline’, *Makivik Corporation*, 2018. https://www.makivik.org/rise-in-the-cost-of-gasoline/ (accessed Dec. 02, 2021).
[5] F.-A. Comeau, J. Raymond, M. Malo, C. Dezayes, and M. Carreau, ‘Geothermal Potential of Northern Québec: A Regional Assessment’, *GRC Transactions (2017)*, vol. 41, pp. 1076–1094.
[6] N. Giordano, I. Kanzari, M. Miranda, C. Dezayes, and J. Raymond, ‘Shallow geothermal resource assessment for the northern community of Kuujjuaq, Québec, Canada’, in *IGCP636 Annual Meeting 2017*, Santiago de Chile, Nov. 2017.
[7] P. Belzile, F.-A. Comeau, J. Raymond, L. Lamarche, and M. Carreau, ‘Arctic Climate Horizontal Ground-Coupled Heat Pump’, vol. GRC Transactions (2017), pp. 1958–1978.
[8] N. Giordano and J. Raymond, ‘Alternative and sustainable heat production for drinking water needs in a subarctic climate (Nunavik, Canada): Borehole thermal energy storage to reduce fossil fuel dependency in off-grid communities’, *Applied Energy*, vol. 252, p. 113463, Oct. 2019, doi: 10.1016/j.apenergy.2019.113463.
[9] N. Giordano, L. Riggi, S. Della Valentina, A. Casasso, G. Mandrone, and J. Raymond, ‘Efficiency evaluation of borehole heat exchangers in Nunavik, Québec, Canada’, in *Proceedings of 25th IIR International Congress of Regrigeration*, Montreal, Canada, Aug. 2019, p. 9. doi: DOI: 10.18462/iir.icr.2019.0547.
[10] J. Meyer, D. Pride, J. O’Toole, C. Craven, and V. Spencer, ‘Ground-Source Heat Pumps in Cold Climates’, May 2011. Accessed: Nov. 24, 2021. [Online]. Available: http://cchrc.org/library/
[11] R. Garber-Slaght, C. Craven, R. Peterson, and R. P. Daanen, ‘Ground Source Heat Pump Demonstration in Fairbanks, Alaska’, Cold Climate Housing Research Center (CCHRC), 2013. Accessed: Nov. 23, 2021. [Online]. Available: http://cchrc.org/library/
[12] T. You, W. Wu, W. Shi, B. Wang, and X. Li, ‘An overview of the problems and solutions of soil thermal imbalance of ground-coupled heat pumps in cold regions’, *Applied Energy*, vol. 177, pp. 515–536, Sep. 2016, doi: 10.1016/j.apenergy.2016.05.115.
[13] H. Qian and Y. Wang, ‘Modeling the interactions between the performance of ground source heat pumps and soil temperature variations’, *Energy for Sustainable Development*, vol. 23, pp. 115–121, Dec. 2014, doi: 10.1016/j.esd.2014.08.004.
[14] W. Yang, L. Kong, and Y. Chen, ‘Numerical evaluation on the effects of soil freezing on underground temperature variations of soil around ground heat exchangers’, *Applied Thermal Engineering*, vol. 75, pp. 259–269, Jan. 2015, doi: 10.1016/j.applthermaleng.2014.09.049.
[15] W. H. Leong, V. R. Tarnawski, and A. Aittomäki, ‘Effect of soil type and moisture content on ground heat pump performance’, *International Journal of Refrigeration*, vol. 21, no. 8, pp. 595–606, Dec. 1998, doi: 10.1016/S0140-7007(98)00041-3.
[16] T. You, W. Shi, B. Wang, W. Wu, and X. Li, ‘A new ground-coupled heat pump system integrated with a multi-mode air-source heat compensator to eliminate thermal imbalance in cold regions’, *Energy and Buildings*, vol. 107, pp. 103–112, Nov. 2015, doi: 10.1016/j.enbuild.2015.08.006.
[17] L. Dai, S. Li, L. DuanMu, X. Li, Y. Shang, and M. Dong, ‘Experimental performance analysis of a ground source heat pump system under different heating operation modes’, *Applied Thermal Engineering*, vol. 75, pp. 325–333, Jan. 2015, doi: 10.1016/j.applthermaleng.2014.09.061.

[18] C. Naranjo-Mendoza, M. A. Oyinlola, A. J. Wright, and R. M. Greenough, ‘Experimental study of a domestic solar-assisted ground source heat pump with seasonal underground thermal energy storage through shallow boreholes’, *Applied Thermal Engineering*, vol. 162, p. 114218, Nov. 2019, doi: 10.1016/j.applthermaleng.2019.114218.
[19] E. Kjellsson, G. Hellström, and B. Perers, ‘Optimization of systems with the combination of ground-source heat pump and solar collectors in dwellings’, *Energy*, vol. 35, no. 6, pp. 2667–2673, Jun. 2010, doi: 10.1016/j.energy.2009.04.011.
[20] E. Kjellsson and Lunds universitet, *Solar Colletors Combined with Ground-Source Heat Pumps in Dwellings - Analyses of System Performance*. 2016. Accessed: Dec. 10, 2021. [Online]. Available: https://portal.research.lu.se/en/publications/
[21] N. Zhu, J. Wang, and L. Liu, ‘Performance evaluation before and after solar seasonal storage coupled with ground source heat pump’, *Energy Conversion and Management*, vol. 103, pp. 924–933, Oct. 2015, doi: 10.1016/j.enconman.2015.07.037.
[22] E. Nordgård-Hansen, N. Kishor, K. Midttømme, V. K. Risinggård, and J. Kocbach, ‘Case study on optimal design and operation of detached house energy system: Solar, battery, and ground source heat pump’, *Applied Energy*, vol. 308, p. 118370, Feb. 2022, doi: 10.1016/j.apenergy.2021.118370.
[23] ‘Simulation énergétique des bâtiments (SIMEB): données météo’, *SIMEB*. https://www.simeb.ca/ (accessed Mar. 17, 2022).
[24] ‘NSRDB data viewer’, *NSRDB: National Solar Radiation Database*. https://nsrdb.nrel.gov/ (accessed Mar. 17, 2022).
[25] CEN 2020, ‘Climate station data from Whapmagoostui-Kuujjuarapik Region in Nunavik, Quebec, Canada, v. 1.5 (1987-2019)’, *Nordica D4*. https://www.cen.ulaval.ca/nordicanad/dpage.aspx?doi=45057SL-EADE4434146946A7 (accessed Jan. 12, 2022).
[26] N. C. Lovvorn *et al.*, ‘ASHRAE Guideline 14-2002: Measurement of Energy and Demand Savings’.
[27] P. Belzile, L. Lamarche, F.-A. Comeau, and J. Raymond, *Revue technologique: efficacité énergétique et énergies renouvelables au nord du Québec : rapport final*. 2017. Accessed: Nov. 17, 2021. [Online]. Available: https://espace.inrs.ca/id/eprint/5308/
[28] Geostar, ‘SYCAMORE SERIES SPECIFICATION CATALOG’. Jan. 2017. Accessed: Oct. 01, 2020. [Online]. Available: https://www.geostar-geo.com/downloads/literature/SC2700AG.pdf
[29] CANADIAN SOLAR INC., ‘PV Module Product Datasheet I V5.0_EN, Quartech CS6P-250/255/260P’. Dec. 2014. Accessed: Feb. 01, 2020. [Online]. Available: http://www.greensolarsolutions.com.au/media/Datasheet_Quartech_CS6P-P_en.pdf
[30] F.-A. Comeau, N. Giordano, and J. Raymond, ‘Shallow geothermal potential of the northern community of Whapmagoostui-Kuujjuarapik’, INRS, Centre Eau, Terre et Environnement, research report R1927, Apr. 2020. Accessed: Jan. 12, 2022. [Online]. Available: http://espace.inrs.ca/id/eprint/11360
[31] Å. Melinder, *Handbook on indirect refrigeration and heat pump systems*. International Institute of Refrigeration, 2015. Accessed: Dec. 01, 2022. [Online]. Available: https://iifiir.org/en/fridoc/handbook-on-indirect-refrigeration-and-heat-pump-systems-digital-or-4652
[32] A. Nikitin, M. Farahnak, M. Deymi-Dashtebayaz, S. Muraveinikov, V. Nikitina, and R. Nazeri, ‘Effect of ice thickness and snow cover depth on performance optimization of ground source heat pump based on the energy, exergy, economic and environmental analysis’, *Renewable Energy*, vol. 185, pp. 1301–1317, Feb. 2022, doi: 10.1016/j.renene.2021.12.132.
[33] American Society of Heating, Refrigerating and Air-Conditioning Engineers (ASHRAE), ‘32.7.1 Vertical Design’, in *2007 ASHRAE Handbook - Heating, Ventilating, and Air-Conditioning Applications (I-P Edition)*, American Society of Heating, Refrigerating and Air-

Conditioning Engineers (ASHRAE), 2007. [Online]. Available: https://app.knovel.com/hotlink/pdf/id:kt006HAFP2/ashrae-handbook-heating/vertical-design

[34] H. Wang, C. Qi, E. Wang, and J. Zhao, ‘A case study of underground thermal storage in a solar-ground coupled heat pump system for residential buildings’, *Renewable Energy*, vol. 34, no. 1, pp. 307–314, Jan. 2009, doi: 10.1016/j.renene.2008.04.024.

[35] S. M. Lopes, R. Furey, and P. Geng, ‘Calculation of Heating Value for Diesel Fuels Containing Biodiesel’, *SAE Int. J. Fuels Lubr.*, vol. 6, no. 2, pp. 407–418, Apr. 2013, doi: 10.4271/2013-01-1139.

[36] J. Krupa, ‘Identifying barriers to aboriginal renewable energy deployment in Canada’, *Energy Policy*, vol. 42, pp. 710–714, Mar. 2012, doi: 10.1016/j.enpol.2011.12.051.

[37] T. M. Weis, A. Ilinca, and J.-P. Pinard, ‘Stakeholders’ perspectives on barriers to remote wind–diesel power plants in Canada’, *Energy Policy*, vol. 36, no. 5, pp. 1611–1621, May 2008, doi: 10.1016/j.enpol.2008.01.004.

[38] ‘Environmental and Social Impact Assessment Review Report on the Whapmagoostui-Kuujjuaraapik Hybrid Power Plant Project by Kuujjuaraapik Whapmagoostui Renewable Energy Corporation’, Comité d’examen des répercussions sur l’environnement et le milieu social (COMEX), Jun. 2022. Accessed: Jul. 15, 2022. [Online]. Available: https://comexqc.ca/en/fiches-de-projet/centrale-denergie-hybride-de-whapmagoostui-kuujjuaraapik/https://comexqc.ca/en/

[39] B. Lei, Z.-J. Duan, and Y.-T. Wu, ‘Thermodynamic investigations on an integrated heat pump with thermal storage for wind-solar hybrid heating’, *Energy Conversion and Management*, vol. 254, p. 115276, Feb. 2022, doi: 10.1016/j.enconman.2022.115276.

[40] A. D. Chiasson, S. J. Rees, and J. D. Spitler, ‘A Preliminary Assessment of the Effects of Groundwater Flow on Closed-Loop Ground-Source Heat Pump Systems’, *ASHRAE Transactions*, vol. 106, pp. 380–393, 2000.

[41] S. Kimiaei and M. Salmanzadeh, ‘Effects of saturated soil on the lengths of a double U-tube borehole with two independent circuits, a parallel double U-tube borehole and on the power consumption of a GSHP’, *Renewable Energy*, vol. 145, pp. 202–214, Jan. 2020, doi: 10.1016/j.renene.2019.04.152.

[42] S. Kavian, C. Aghanajafi, H. Jafari Mosleh, A. Nazari, and A. Nazari, ‘Exergy, economic and environmental evaluation of an optimized hybrid photovoltaic-geothermal heat pump system’, *Applied Energy*, vol. 276, p. 115469, Oct. 2020, doi: 10.1016/j.apenergy.2020.115469.

Declaration of interests

☒ The authors declare that they have no known competing financial interests or personal relationships that could have appeared to influence the work reported in this paper.

☐The authors declare the following financial interests/personal relationships which may be considered as potential competing interests: